

# Remote sensing of shallow coastal benthic substrates: *in situ* spectra and mapping of eelgrass (*Zostera marina*) in the Gulf Islands National Park Reserve of Canada

Jennifer D. O'Neill<sup>a,\*</sup>, Maycira Costa<sup>a</sup>, and Tara Sharma<sup>b</sup>

<sup>a</sup>Dept. of Geography, University of Victoria, PO Box 3060, STN CSC, Victoria, BC, Canada, V8W 3R4 – (joneill, maycira)@uvic.ca

<sup>b</sup>Parks Canada, Gulf Islands National Park Reserve of Canada, 2220 Harbour Road, Sidney, BC, V8L 2P6 – Tara.Sharma@pc.gc.ca

**Abstract** - Eelgrass (*Zostera marina*) is a keystone component of coastal ecosystems. However, anthropogenic pressures have caused community decline worldwide. Delineation and continuous monitoring of eelgrass distribution is an integral part of understanding these pressures and effectively managing them. A proposed tool for monitoring is remote imagery. However, to apply this technology, an understanding is required of the spectral behavior submerged coastal substrates. In this study, *in situ* above-water hyperspectral measurements were used to define key spectral variables providing greatest separation between *Z. marina* and associated substrates. The selected variables were: slope500-530nm, first derivatives ( $R'$ ) at 566nm, 580nm, and 602nm, and yielded 98% overall classification accuracy. Classification of a hyperspectral airborne image showed a major advantage of variable selection was meeting band sample size requirements of the maximum likelihood classifier, which yielded classification accuracies of over 85%.

**Keywords:** eelgrass; seagrass; *in situ* spectra; remote sensing; hyperspectral; feature selection

## 1. INTRODUCTION

Eelgrass (*Zostera marina*) is a vital component of inter- and sub-tidal ecosystems. Widely recognized for its ecological and conservation value, it provides shoreline stability (Fonseca & Cahalan, 1992), mediates biochemical balance in the immediate and broader ecosystem (Apostolaki, 2010), and provides a fundamental nursery ground and food source for a variety of marine organisms (Borg et al., 2006). Populations, however, have experienced worldwide decline. An estimated 2–5% of seagrass ecosystems are lost annually due to anthropogenic pressures, both direct (development and recreation) and indirect (climate change and light limiting effects of activities such as aquaculture, upland activities, and pollution) (Apostolaki et al., 2009). Loss is projected to accelerate as human pressure grows. Therefore, a baseline and continued monitoring of eelgrass distribution is exceedingly important in mitigating additional loss and managing existing meadows. A proposed tool for such monitoring is remote imagery, which can cost- and time- effectively cover large and inaccessible areas frequently (Dekker et al., 2005). However, effective application of this technology requires an understanding of the spectral behaviour of eelgrass and associated substrates.

The spectral properties of submerged substrates are influenced not only by their mineral and pigment components and the properties of water column, but also by the characteristics of the remote sensor. High spatial and spectral resolutions offer greater discernibility of spatial and spectral detail, but at the expense of processing time due to large data volumes. Data reduction methods address this issue by removing redundant variables and retaining those offering the greatest distinction between substrates (Richards & Jia, 2005). In this light, the goal of this study was two-fold: (1) to use *in situ* hyperspectral measurements to identify bands or bands indices (hereafter called spectral variables) which

maximize spectral separation of eelgrass from other substrates and (2) to test the identified variables in image classification.

## 2. METHODOLOGY

### 2.1 Study Area

This research took place at Sidney Spit, a 1.78km<sup>2</sup> protected marine area on the north-eastern extreme of Sidney Island, British Columbia, Canada, which encompasses a 1.8 km long sand spit and shallow lagoon and is protected within the Gulf Islands National Park Reserve of Canada (GINPRC) (Figure 1). The major submerged substrates present at the site were eelgrass (*Zostera marina*), green algae (*Ulva fenestrata*, *Enteromorpha* spp., and filamentous green algae), sand, sea asparagus (*Salicornia virginica*) and small patches of brown algae (*Fucus* spp., *Sargassum muticum*, and *Laminaria saccharina*).

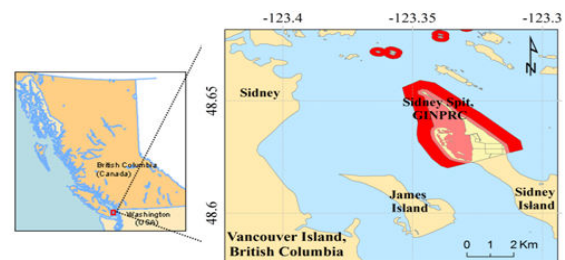


**Figure 1.** Sidney Spit, Sidney Island, BC, is part of the Gulf Islands National Park Reserve of Canada (GINPRC). Pale red area is Marine protected area within the park; dark red is Marine Extension area.

Measurement of water biophysical conditions at the time of spectral sampling revealed the following characteristics: temperature (avg = 11.5 °C); salinity (29 ppt); total suspended material, TSM (4.03 g m<sup>-3</sup>); total organic carbon, TOC (47.60%); absorption by chromophoric dissolved organic material,  $a_{CDOM}$  (0.24 m<sup>-1</sup>); and Chl-*a* (2.44 mg m<sup>-3</sup>); clearly characterizing a case 2 water type (O'Neill, 2011). The relative magnitude of measured  $K_d$  values was related to the distribution of the water constituents. Characteristic blue absorption by CDOM, blue and red absorption by Chl-*a* and red scattering by total suspended matter (TSM) caused higher  $K_d$  values in those ranges and lowest  $K_d$  (~0.4 m<sup>-1</sup>) in the green range.

### 2.2 Data Acquisition

Initially, substrate ground-truth was conducted by photograph, description of substrate type and percent cover (plus shoot density in the case of eelgrass), and GPS for a total of 387 sites from June through August 2008, and then further in July 2010 (120 additional sites). On August 14-18 and 31, 2008, *in situ* above-water spectra were collected from onboard a small motor vessel. The following data were collected at each of these field sites: (1) GPS location; (2) above water photos and underwater videography for substrate identification and density estimation; (3) depth; (4) wind speed to correct radiometric measurements for stray light

added by the water surface; and (5) above-water hyperspectral measurements for spectrally characterizing submerged substrates.

Above-water *in situ* radiance spectra (N=49) were measured over the four major substrates, eelgrass (*Z. marina*) (n=25), green algae (*U. Fenestrata* and *Enteromorpha sp.*) (n=8), sand (n=9), and deep water (>30 metres) (n=7). Total water leaving radiance ( $L_T(\lambda)$ , 40° from nadir) and sky radiance ( $L_{sky}(\lambda)$ , 40° from zenith) were measured one metre above the water surface using a Satlantic HyperSAS mounted on a tripod in the boat. The radiance sensors had a half-angle FOV of 3°, two-nanometre spectral resolution and a spectral range of 350 - 800nm. Total irradiance ( $E_s(\lambda)$ , cosine collector at zenith) was measured with a Satlantic OCR-3000 sensor (Satlantic, 2003). Spectral were acquired continuously (every two seconds) for a period of 40 seconds, for 20 spectra per site, while effort was made to maintain a  $L_T$  sensor viewing geometry of 90° from the sun to avoid specular reflection (Mobley, 1999). All measurements were made in clear weather with less than 20% cloud cover, low wind speeds (<10 ms<sup>-1</sup>), and solar zenith between 30-60° (Hooker *et al.*, 2004).

Sun glint outliers were removed from the  $L_T$  spectra following Hooker *et al.*, (2002). The remaining radiance measurements were converted to above-water remote sensing reflectance ( $R_{rs}(\lambda)$ ) using the modified Fresnel reflectance glint correction algorithm S95 of Ruddick *et al.*, (2006) and then averaged. To correct a vertical offset error inherent in each spectra due to the slight variability of  $\rho'$  between acquisitions, each spectrum was offset by a value equal to the mean reflectance value from 750-800nm, standardizing each spectrum to a NIR value of zero in this range.

After spectra corrections, six benthic classes were defined based on substrate type and depth: deep water (dW)(>30m), deep sand (dS) and deep eelgrass (dE) (>3m); shallow sand (sS), shallow eelgrass (sE) and shallow green algae (sAg)(<3m). No green algae sites could be found deeper than three metres and so representative spectra are absent. The three metre threshold was defined because depth stratification has been shown to improve classification accuracy (Phinn *et al.*, 2005) and preliminary analysis of reflectance spectra showed noticeable magnitude differences beyond this depth, particularly at 700-750 nm.

### 2.3 Data Reduction and Variable Selection

To identify major spectral variables in the *in situ* spectra, three methods were employed. First, major reflectance features were identified by visual examination of the class spectral means. Second, the exact locations ( $R'\lambda$ ) of these features were identified as zero values in the first derivative spectra. It has been observed that while spectral magnitude of a single substrate can be variable, spectral shape is typically retained (Vahtmae *et al.*, 2006). To account for spectral shape, the third step involved calculating the ratios and slopes (denoted  $\lambda:\lambda$  and  $s\lambda-\lambda$ ) between the features identified in first derivative analysis, for a total of 23 indices. All first derivative values and 14 published vegetation indices were added to the list for a total of 388 spectral variables.

A two step statistical reduction was then used: M-statistic (Kaufman and Remer, 1994) followed by discriminant analysis (DA). The M-statistic was calculated for each variable of all cases of eelgrass-other substrate class pairing (i.e. eelgrass-sand) following Kaufman and Remer (1994), where  $M > 1.0$  indicated good class separation and  $M < 1.0$  indicated poor separation. The variables with the highest M-statistic values were retained, and termed "Set 1." In the second step, a DA with stepwise variable selection was run on the Set 1 variables to eliminate remaining redundancy, yielding "Set 2," the minimum variable set with the

maximum discriminating ability (Bandos *et al.*, 2009). A Set 2 was derived for each of the following separability cases: shallow substrates (< 3m), deep substrates (> 3m), and both shallow and deep substrates together. The classification accuracy of each Set 2 was evaluated by applying the derived DA model to the dataset with leave one out cross-validation and 500 bootstrap samples stratified by substrate at a confidence level of 95%.

### 2.4 Classification of hyperspectral airborne image

The reduced variable set (Set 2) derived from the previous steps was further tested on hyperspectral imagery. Supervised classification algorithms were applied to an AISA hyperspectral airborne image acquired over Sidney Spit by Terra Remote Sensing on August 16, 2008 at 12:14 during low tide (0.42m), with a spatial resolution of 2x2m, spectral resolution of 2 nm and spectral range of 408 - 2494nm. Prior to classification, the six flight lines were geometrically corrected with Hyperbatch, a custom software developed by the Hyperspectral and LiDAR Research Group at the University of Victoria. The flight lines were geographically matched to one another manually to minimize residual geo-locational error (RMSE = 0.60m), and then mosaicked together. A land mask was defined as DN(450nm) > 2200 and a Gaussian spectral smoothing window of 10 nm was applied to each pixel to remove spectral noise. Empirical line calibration (ELC) atmosphere correction was performed with one deep water site and one shallow sand site as input, and corrected for surface glint following Hedley *et al.* (2005). Optically deep water was masked with a threshold of 5.5 metres, which was the eelgrass detectability threshold of the AISA sensor at 566 nm following Dekker *et al.* (2005). The resulting image was termed Image 1. Image 1 was reduced to the variable set selected in Section 2.3: s500-530, R'566, R'580, R'602 to create Image 1R.

The minimum distance supervised classifier was applied to both images. The more statistically complex maximum likelihood (ML) classifier was applied only to the variable reduced Image 1R and not to the full spectral resolution Image 1 due to statistical constraints; ML requires the band set to contain less than  $n-1$  bands, where  $n$  is the number of training samples in each substrate class (Bandos *et al.*, 2009). In this study, the 175 bands of the full-resolution spectra greatly exceeded  $n-1$ , as  $n$  varied from 2 to 51.

Approximately 20% of the ground-truth data sites (n= 99) were used for classifier training. The remaining 80% of sites (n= 408) were used in validation of each image to determine eelgrass producer and user accuracies, as well as overall accuracy (Story & Congalton, 1986). The classification scheme was the same as the *in situ* scheme, but with the addition of shallow brown algae (sAb), and exposed sea asparagus (eAsp).

## 3. RESULTS AND DISCUSSION

### 3.1 Spectral characteristics of the benthic substrates

Figure 2 summarizes the above-water reflectance spectra. Eelgrass and its associated substrates were spectrally distinct and the spectral shapes and relative magnitudes were in agreement with reported *in situ* above-water measurements (e.g. Dierssen *et al.*, 2003). Spectral attenuation features of the water column and constituents (as described in Section 2.1) were found in all measured spectra and were more pronounced with water depth. The most marked differences between benthic classes occurred in the green spectral range between 500-600 nm, coinciding with the lowest  $K_d$  values. Within this spectral region, a broad green peak at the photosynthetic pigment absorption minimum between 560 and 575nm was present for all substrates (Figure 2). Green peak

ascending and descending slopes of all classes became steeper with decreasing water depth. Overall, green algae slopes were steeper than those of eelgrass, likely due to epiphyte presence.

The marked absorption feature in the blue range present in all substrates due to CDOM and phytoplankton Chl-*a*, was strengthened in vegetation classes by chlorophyll-*a* and -*b*, and lutein, and by the additional accessory pigment  $\beta$ -carotene in green algae. The other major absorption feature of Chl-*a* and -*b* appeared in the red region at 662-669 nm for all except sand, which occurred at 675nm (Figure 2). The presence of epiphytic diatoms on eelgrass and green algae was signified by a unique Chl-*a* and -*c* absorption trough between 630-640nm and a broad spectral flattening caused by fucoxanthin absorption in the 530-566nm range and physical obstruction of eelgrass green reflectance in the 500-600 nm range (Fyfe, 2003). For all shallow vegetation classes, the red-edge occurred in the range of 670-705nm and a NIR peak occurred between 687 - 710 nm (Figure 2).

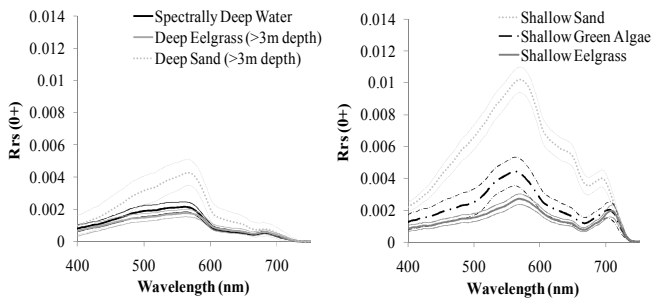


**Figure 2.** Mean above-water substrate reflectance and 95% CI.

### 3.2 Spectral variable selection

The M-statistic generally defined higher values for the first derivative variables and indices, suggesting that spectral shape was more effective at substrate separation than reflectance magnitude. Shallow water Set 2 variables were s500-530, R'566, R'580, and R'602 for a total classification accuracy of 97%. The only misclassification was of one (out of eight) green algae sample classified as shallow eelgrass. Deep water Set 2 variables were s500-530, R'580, and R'602 for a total classification accuracy of 100%. Caution should be taken in interpreting this result as the sample size of deep eelgrass was small ( $n = 4$ ). The Set 2 variables for each depth group were pooled to test their combined efficacy in a single classification. The stepwise DA retained all four variables in the model for a total classification accuracy of 98%, misclassifying the same green algae sample as shallow eelgrass. The retained high accuracy for combined depths suggests that if these variables were used to classify a remotely sensed image, it would not be necessary to stratify by depth. Set 2 variables for the combined depths, derived from the discriminant analysis, are reported with M-statistic values in Tables 1 and 2.

**Table 1.** Set 2 showing spectral separability of shallow eelgrass (<3m) from other substrates. The numerical values are the M-statistic results; a shaded box represents good separability ( $M > 1$ ).

Band	sS	sAg	dE	dS	dW
s500-530	5.73	1.63	1.90	0.49	1.76
R'566	0.56	1.40	2.51	0.68	2.80
R'580	2.10	1.64	0.33	3.21	1.05
R'602	5.70	0.64	0.56	2.46	0.25

**Table 2.** Set 2 showing spectral separability of deep eelgrass (>3m) from and other substrates. The numerical values are the M-statistic results; a shaded box represents good separability ( $M > 1$ ).

Band	sS	sAg	sE	dS	dW
s500-530	11.45	2.91	1.90	4.55	0.09
R'566	1.62	0.56	2.51	1.47	1.10
R'580	3.86	2.93	0.33	6.60	2.10
R'602	8.93	1.19	0.56	4.22	0.26

To calculate these variables in an image, one would require ten bands of 4 nm bandwidth: R500, R530, R554, R568, R578, R582, R600, R604, R668, R710 nm. These bands are in agreement with Fyfe's (2003) guidelines for an appropriate seagrass classification band set as they are narrow and do not overlap. They target the peak (R'566) and shoulders (s500-530 & R'580) of the green reflectance maxima, the red absorption feature (R'602), and the epiphyte reflectance region (R'580). However, while Fyfe's recommendations are based on reflectance, this study selected measures of reflectance, which capture spectral shape.

Image classification accuracy should be robust to atmospheric interference because the variable set is independent of the blue wavelengths, where atmospheric interference is greatest. It may not, however, be robust for more turbid waters; as turbidity increases, light attenuation in the water increases, causing the maximum depth of eelgrass detection to become shallower. Therefore imagery should always be acquired at the lowest possible tide and at slack tide to avoid resuspension of particles.

### 3.3 Classification of hyperspectral airborne image

Of the two processing approaches used on the AISA image, the glint and atmospheric corrected (ELC) reduced variable image (1R) showed the best results. MD classification of the full-resolution Image 1 yielded eelgrass producer/user accuracies of 74%/ 86% for shallow (< 3 m) and 72%/ 90% for deep (> 3 m) eelgrass; overall accuracy was 63%. Error occurred primarily between sE-sAg and dE-dS. Approximately 11% of all sAg sites were misclassified as sE (producer error), while 14% of all pixels classified as sE were actually sAg and 29% of all dE sites were misclassified as dS (user error). MD classification of the reduced variable Image 1R yielded much lower accuracies: 20%/ 45% for shallow (< 3 m), 59%/ 59% for deep (> 3 m) eelgrass, and 24% overall accuracy. This was due to considerable confusion between shallow eelgrass (sE) and other green vegetation; 62% of all sE training sites were misclassified as eAsp, while 38% of all pixels classified as sE were actually sAg testing sites. In deep water, there was 40% user and 39% producer error between dE and dS.

However, when ML classification was applied to Image 1R, accuracy increased considerably to 85%/ 96% for shallow (< 3 m) and 98%/ 93% for deep (> 3 m) eelgrass; overall accuracy was 83%. The substrate map produced by this best classification is shown in Figure 3. The major source of confusion was between sE and sAg. About 5% of all sAg training sites were misclassified as sE (producer error) while 14% of all pixels classified as sE were actually sAg (user error). The sand class resulted in the least confusion at all depths, with 2% producer error at all depths. This confusion was mainly near the periphery of the eelgrass bed where sparse density and georeferencing error likely play a role.

This result emphasizes the importance of variable reduction because the full-resolution hyperspectral data had too many variables to allow the more statistically complex maximum

likelihood classification (Bandos et al., 2009). The results obtained with a minimum distance classifier were inferior, especially when using the variable reduced band set (20% overall accuracy), suggesting that the Euclidian distance measurements used in the MD algorithm required a larger set of input bands to improve the classification or that the variable reduction approach eliminated variables containing important information about substrate separability. It is also possible that factors are not accounted for in the *in situ* spectra that are present in the image – a possibility supported by the lower classification accuracy even of the best image classification compared with *in situ* accuracy values. These factors include (1) higher spatial heterogeneity within the 2x2m image pixel compared with the *in situ* field of view, (2) lower substrate certainty due to combined locational errors of the GPS and image georeferencing, and (3) greater noise introduced by correcting a 1 km airborne atmospheric path, compared with 1 m *in situ*. Such effects would likely be greater in satellite imagery, such as IKONOS or Quickbird.

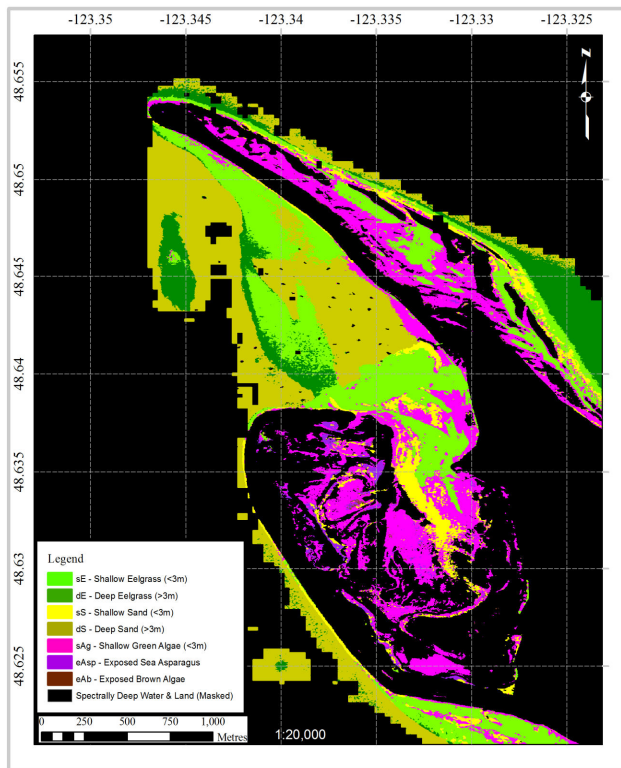


**Figure 3.** Most accurate eelgrass map produced in this study: ML classification of: s500-530, R'566, R'580 and R'602. Eelgrass producer/user accuracies were 85%/ 96% for shallow and 98%/ 93% for deep eelgrass. Overall accuracy was 83.2%.

## 5. CONCLUSIONS

The key wavelengths identified in this study are recommended for application with analysis of airborne and satellite imagery when the goal is delineating the spatial distribution of eelgrass. These maps could be used as baseline inventory data and, when merged with other ancillary data layers could be used to report on the structure and functioning of coastal ecosystems. However, it should be noted plant phenology, water properties and substrate types inevitably vary over time and between locations and it is therefore recommended that this variable set be tested on data gathered at Sidney Island over different seasons and at additional

areas in the Gulf Islands National Park to confirm whether these models are local- and time-specific, or more widely applicable.

## Acknowledgements

The authors would like to acknowledge staff at Parks Canada for logistics and technical support, student volunteers for help with field work, Terra Remote Sensing for image acquisition, and the Hyperspectral & LiDAR Research Group at UVic of Dr. Olaf Niemann for radiometric and Hyperbatch geometric correction of imagery. Funding sources were NSERC and CFI / BCKDF.

## References

- E. Apostolaki, N. Marba, M. Holmer, I. Karakassis. "Fish farming enhances biomass and nutrient loss in *Posidonia oceanica* (L.)," *Estuar. Coast. Shelf. S.*, vol 81, p.p. 390–400, 2009.
- J. Borg, A. Rowden, M. Attrill, P. Schembri, M. Jones. "Wanted dead or alive: high diversity of macroinvertebrates associated with living and "dead" *Posidonia oceanica* matte," *Mar. Biol.* vol 149(3), p.p. 667-677, 2006.
- T. Bandos, L. Bruzzone, G. Camps-Valls. "Classification of hyperspectral images with regularized linear discriminant analysis," *IEEE T. Geosci. Rem.* vol 47(3), p.p 862-873, 2009.
- A. Dekker, V. Brando, J. Anstee. "Retrospective seagrass change detection in a shallow coastal tidal Australian lake," *Remote Sens. Environ.* vol 97, p.p. 415–433, 2005
- H. Dierssen, R. Zimmerman, R. Leathers, T. Downes, C. Davis. "Ocean color remote sensing of seagrass and bathymetry in the Bahamas Banks by high-resolution airborne imagery," *Limnol. Oceanogr.* vol 48(1), p.p. 444-455, 2003
- S. Fyfe. "Spatial and temporal variation in spectral reflectance : Are seagrass species spectrally distinct?" *Limnol. Oceanogr.* vol 48(1), p.p. 464-479, 2003.
- M. Fonseca, J. Cahalan. "A preliminary evaluation of wave attenuation by four species of seagrass," *Est Coast Shelf Sci*, vol 35(6), p.p. 565-576, 1992.
- J. Hedley, A. Harborne, P. Mumby. "Simple and robust removal of sun glint for mapping shallow-water benthos," *Int. J. Remote Sens.* vol 26, p.p. 2107-2112, 2005.
- S. Hooker, G. Zibordi, J. Brown. "Above-water radiometry in shallow coastal waters," *Appl. Opt.* 43(21), p.p. 4254-68, 2004
- Y. Kaufman, L. Remer. "Detection of forests using mid-IR reflectance: An application for aerosol studies," *IEEE T. Geosci. Remote.* vol 32(3), p.p. 672-683, 1994.
- C. Mobley. "Estimation of the Remote-Sensing Reflectance from Above-Surface Measurements," *Appl Opt*, 38, 7441-55, 1999.
- J. O'Neill. "Mapping of eelgrass (*Zostera marina*) at Sidney Spit, Gulf Islands National Park Reserve of Canada, using high spatial resolution remote imagery," *MSc Graduate Student Thesis, University of Victoria*, 2010.
- S. Phinn, A. Dekker, V. Brando, C. Roelfsema. "Mapping water quality and substrate cover in optically complex coastal and reef waters: An integrated approach," *Mar. Pollut. Bull.* vol 51, p.p. 459–469, 2005.
- J. Richards, X. Jia. Ch 10: *Feature Reduction*. In: Remote sensing digital image analysis: an introduction. 4<sup>th</sup> Ed., Springer, 2006.
- K. Ruddick, V. Cauwer, Y. Park, G. Moore. "Seaborne measurements of near infrared water-leaving reflectance: The similarity spectrum for turbid waters," *Limnol.Oceanogr.* vol 51(2), 1167-1179, 2006.
- Satlantic Inc. "Operation manual for the HyperSAS," *Satlantic Document #SAT-DN-00212, Revision A*, 2003.
- M. Story, R. Congalton. "Accuracy Assessment: A User's Perspective," *Photogramm. Eng. Rem. S.* 52(3), 397-399, 1986.